MDPI

Article

Deciphering the Regulatory Mechanism of PmMYB21 in Early Flowering of *Prunus mume* through Dap-Seq and WGCNA Analysis

Xi Yuan [1,2], Ran He [1], Hui Zhang [1], Dongyan Liu [1], Donghuan Liu [1], Zhihong Niu [1], Yu Zhang [1,*] and Xinli Xia [2,*]

[1] Beijing Botanical Garden, Key Laboratory of National Forestry and Grassland Administration on Plant Ex Situ Conservation, Beijing Floriculture Engineering Technology Research Centre, Beijing 100093, China; cc_yuan@126.com (X.Y.)

[2] State Key Laboratory of Tree Genetics and Breeding, National Engineering Research Center of Tree Breeding and Ecological Restoration, College of Biological Sciences and Technology, Beijing Forestry University, Beijing 100083, China

* Correspondence: zhangyu@chnbg.cn (Y.Z.); xiaxl@bjfu.edu.cn (X.X.); Tel.: +86-138-118-60926 (Y.Z.); +86-135-819-19075 (X.X.)

Abstract: *Prunus mume* Siebold & Zucc (mei) is a horticulturally important fruit tree that undergoes anthesis in winter. Therefore, its flowering process is challenged by low-temperatures conditions. The transcription factor (TF) MYB21 is pivotal in regulating the flowering process, and particularly functions in petal expansion and filament elongation. However, the regulatory mechanism of PmMYB21 in mei remains unknown. To breed early-flowering cultivars, a deeper understanding of PmMYB21-regulated genes is essential. We employed DNA affinity purification sequencing (Dap-seq) to identify downstream genes bound by PmMYB21. The results revealed the promoter region is the primary binding region of PmMYB21, and the AGTTAGGTARR motif (motif1) is the predominant binding sequence type. Our analysis identified 8533 genes that are potentially bound by PmMYB21 with the motif1 sequence type, within the promoter region. These genes are involved in biological processes critical to flowering. Further refinement of candidate genes was achieved through Weighted Gene Co-expression Network Analysis (WGCNA), which identified the co-expressed genes of *PmMYB21* during flowering activity. Integrating Dap-seq and WGCNA data, we narrowed down the candidate gene list to 54, with a focus on 4 MADS-box genes and 2 hormone signaling genes that are crucial to the flowering process under low-temperature conditions. This study offers valuable insights into the molecular underpinnings of PmMYB21's role in the low-temperature flowering regulation of mei, paving the way for the development of new cultivars adapted to early blooming.

Keywords: *Prunus mume*; PmMYB21; Dap-seq; WGCNA; flowering; low temperature

1. Introduction

Prunus mume (hereafter referred to as mei) is a member of the Rosaceae, and is a traditional ornamental tree in China [1]. Flower buds form in summer and flowering occurs in winter or the early spring of the following year. Flower buds begin to expand when the temperature is 4 °C and anthesis occurs at 13 °C [2]. As a result of the initiation of flowering at low temperatures, mei often blooms when snow occurs in early spring, a phenomenon that is loved by the public. Therefore, early flowering became an important breeding objective of mei cultivars.

The flower buds of mei need to overcome the endodormancy by low temperature in the autumn and winter, and then enter the ecodormancy period to constantly sense temperature changes to regulate the flowering process in early spring. Although there are many horticulturally important fruit trees of Rosaceae having the same flower development process in the annual growth cycle, such as apple, cherry, peach, and almond, the research

focus is mostly on endodormancy [3–5], and little attention is paid to the flowering process after endodormancy release. On the other hand, the regulation mechanism of flowering has been well studied in annual herbs, such as *Arabidopsis thaliana*. However, it is difficult to screen the key genes in petal expansion and stamen filament elongation, because their bud differentiation overlaps with the organ extension in the late flowering process.

In order to support efforts to develop cultivars that will flower even earlier, we need better understanding of why mei flowers so early. Our previous studies have shown that the bud's constant efforts to grow under low temperatures during the ecodormancy period ultimately lead to the early-flowering phenotype of mei in Beijing [2]. This suggests that the key to early flowering lies in the response of a group of flowering-related genes at low temperature during the ecodormancy state in mei. We then found a TF that is closely related to the flowering process of mei, named PmMYB21. The expression level of PmMYB21 was significantly up-regulated with the progression of flowering in mei cultivars. Additionally, the up-regulated timing of the PmMYB21 expression level in early-flowering cultivars was significantly earlier than that in late-flowering cultivars [6]. Interestingly, we have highlighted that in mei there is only one homologous gene of subgroup 19 of R2R3-MYB, PmMYB21 [6,7]. This may suggest that the flowering process, which regulates redundancies by AtMYB21/24/57 in *Arabidopsis thaliana* [8–12], is regulated by only one gene in mei. We believe that this characteristic makes mei an intriguing material for studying the regulatory function of MYB21 during the flowering process. In the absence of reports on MYB21 downstream genes in model plants, analysis and screening of the downstream genes of PmMYB21 are of great significance to explain the flowering process.

The genome serves as the genetic landscape that outlines the potential for various traits, including the timing and characteristics of flowering in plants. Dap-seq identifies the plant genomic fragments that interact with the protein in vitro. Dap-seq reflects all the binding possibilities of the TF and enables the regulatory relationships of genes to be inferred [13]. On the other hand, the transcriptome provides data of the gene expression level in particular tissues, development stages, and environmental conditions. There are reports of using the combination of RNA-seq and DAP-seq to screen key candidate genes for the peach harvest date from differentially expressed genes (DEGs) between early and late harvest cultivars, and attempts to describe the regulatory relationships among them [14]. The integrative approach of these two datasets allows us to understand not only which genes are involved in the process, but also how their expression is modulated to drive the complex developmental program.

In this study, we used Dap-seq to discover the binding site of PmMYB21 and analyzed the binding genes. Considering that Dap-seq is a statistical study of binding potential at the DNA level, we also used WGCNA to classify a pair of cleverly designed transcriptome data to obtain the co-expressed genes of *PmMYB21*. By overlapping the genesets obtained from Dap-seq and WGCNA, we further narrowed down the candidate genes, and screened out key genes closely related to flowering which are regulated by PmMYB21 with high potential. Our results are conducive to the future exploration and verification of the downstream genes of PmMYB21, provide a strong basis for the development of flowering time molecular markers, and increasing the efficiency of tree breeding programs.

2. Materials and Methods

2.1. Plant Material

Two mei cultivars, "Fenhong Zhusha" ("FZ") and "Zao Lve" ("ZL"), were used in this study. Both cultivars were grafted on *Prunus davidiana* rootstocks. One tree per cultivar was used in the experiment. To reflect the bud developmental state of the whole plant, all buds on two twigs of each branch from three different sides of each experimental tree were collected as one biological replicate. Three biological replicates constituted one sample. We took the S2/S4/S6/S8 bud development stage as the dominant stage [2], and selected four samples of "FZ", and five samples of "ZL" from 9 January to 13 March in 2019 (Table S1).

The collected buds were quickly put into liquid nitrogen and then brought back to the laboratory and stored in an ultra-low temperature refrigerator at $-80\ ^\circ$C for use.

2.2. Growth Conditions

All plants used in our study were planted within 15 m of each other, on the same hillside without shade around, in the Jiufeng International Mei Garden ($40^\circ03'53''$ N; $116^\circ05'49''$ E; 132 m a.s.l.), Beijing, China. The artificial horticultural conditions for each plant cultivars were the same.

2.3. PmMYB21 Full-Length CDs Clone

After grinding flower buds with liquid nitrogen, total RNA was extracted using an OMEGA R6827 Plant RNA kit (OMEGA Bio-tek Inc., Norcross, GA, USA) according to the instructions. R312 kit (Novozan Biotechnology Co., Ltd., Beijing, China) was used to reverse transcribe the first strand of cDNA. The double-ended primer of *PmMYB21* with the Super1300 arm was designed according to *Prunus mume* genome information (Table S2). *PmMYB21* was recombined to the Super1300 vector using C114 kit (Novozan Biotechnology Co., Ltd., Beijing, China) according to the operating manual, and then transferred to DH5α *Escherichia coli* for propagation and sequencing. After analysis and verification, the target sequence was obtained.

2.4. Dap-Seq and Data Analysis

Among the many methods for identifying downstream genes, DAP-Seq mines downstream genes through in vitro binding and high-throughput sequencing techniques [15], and is suitable for plant materials without a regeneration and genetic transformation system [16], such as mei.

The *PmMYB21* CDs sequences of the two mei cultivars were exactly the same [6]. The genomics DNA was extracted from the S6 flower bud of mei using the CTAB method to prepare the DNA library. The CDS of *PmMYB21* was inserted into the HaloTag expression vector to generate recombinants. In two replicates, Halo-PmMYB21 was co-incubated with the DNA library, while the mixture of HaloTag and the DNA library served as the blank control. The DNA fragment that bound to PmMYB21 was eluted and then sequenced on an Illumina NovaSeq 6000 platform. Fastp was used to filter raw data to obtain high-quality sequencing data and clean reads for downstream analysis [17]. The clean reads were aligned to the *Prunus mume* reference genome using BWA-MEM v2.2.1 [18]. Dap-seq was performed by Yongji Biotechnology Co. Ltd., Guangzhou, China.

The 2k bp long promoter region before the Transcription Start Site (TSS) is generally considered to be a key region in regulating gene expression. We used MACS callpeak [19], and the types of gene regions where the peak is located were counted and displayed using a pie chart. The typical motifs in the peak region were picked up by MEME-ChIP [20]. Annotation peaks were detected with ChIPseeker software v1.34.1 [21]. The GOseq R soft package was used for Gene Ontology (GO) enrichment analysis of DEGs that were aligned with GO (p-value < 0.05) [22]. The genes with binding sites in the promoter region were enriched and analyzed to extract the genes related to flowering.

2.5. RNA-Seq and WGCNA

Total RNA of 9 flower bud samples was extracted. The libraries were sequenced on the Illumina Hiseq 6000 platform to generate 150 bp paired-end clean bases not less than 9 G. Using the FPKM (Fragments Per Kilobase of exon model per Million mapped fragments) value as basic data for WGCNA [23], the threshold was set to fpkm > 5 in 60% samples.

Two cultivars of mei had different flowering stages under the same date, but all completed the same flowering process. This means that genes associated with flowering undergo similar trends in transcript expression under different environmental conditions. Based on this, we selected flower buds from four representative stages of the flowering process for transcriptome sequencing. The phenotypic data corresponding to the samples

were used as the basis for correlation analysis of the divided modules. Finally, gene modules that prefer the flowering stage to environmental changes were selected as the key modules related to flowering.

2.6. Quantitative Real-Time-PCR Validation

qRT-PCR was performed on the CFX96 TouchTM RealTime PCR Detection System (Bio-Rad, Hercules, CA, USA). The parameters, internal control genes, and method of specific primer design were the same as in our previous paper [24]. The transcription levels were determined using the $2^{-\triangle\triangle Ct}$ method. The specific primers are listed in Table S2.

2.7. Candidate Gene Screening

In order to select downstream genes of PmMYB21 that are more likely to be involved in flowering, we used the two genesets obtained by Dap-seq and WGCNA to screen candidate genes by overlapping them with Venn analysis in TBtools software 2.042 [25]. We also annotated the located regions (within 1 kb or 1–2 kb promoter) and significance (FDR) in the promoter region of candidate genes.

2.8. Heat Map of Candidate Genes

For further information about the key candidate genes, the FPKM values in flower buds during flowering of candidate genes were used to make heat maps using the heatmap option in TBtools software 2.042 [25], normalized to the row.

3. Results

3.1. The Genes Bound by PmMYB21 Are Enriched in the Flowering Process

To determine the regulatory function of PmMYB21 in the flowering process of mei, DAP-seq was used. The raw data of Dap-seq were not less than 4 G. Among them, clean data accounted for more than 98%. Q20 and Q30 of clean data were above 97% and 92%, respectively. The filter ratio was above 99%. The mapping rate also reached over 97% (Table S3). In turns of the PmMYB21 binding region, 27,478 peaks were in the confidence interval, accounting for 77.9% of the total number of detected peaks (Figure 1a). The sequencing results are highly reliable for their stability and good repeatability.

A total of 35,293 peak were identified. Among them, 14,299, 9364, 6180, 4926, and 524 peaks were located in distal intergenic, promoter, intronic, exon, and downstream regions, respectively (Table S3). This indicates that the promoter is the crucial binding region of the PmMYB21 protein, except the distal intergenic region (Figure 1b).

A total of 19,821 genes can be bound by PmMYB21. Among them, the AGTTAG-GTARR motif was the most dominant recognition sequence type (Figure 1c), involving 19,663 genes (99.2% of the total). There were 8533 genes bound with this sequence type in the promoter region, accounting for 43.4% of 19,663 genes. GO enrichment analysis showed that these genes were mainly enriched in biological processes related to hormone regulation, flower development, and cell wall modification. A total of 374 genes are closely related to the process of flower development. These genes were enriched in 26 flowering-related biological processes, including 2 in photoperiod, 6 in flower development, 6 in stamen development, 7 in fertilization, 3 in embryo or seed development, and 2 in fruit-related biological processes (Figure 1d). This result is consistent with our focus on the biological processes of mei.

Among them, 211 genes involved in 11 flowering-related biological processes (Table S4) were selected to form a geneset (Table S5) for further candidate gene screening.

3.2. The Co-Expression Gene of PmMYB21

Transcriptome sequencing of nine samples of two mei cultivars obtained raw data not less than 8.9 G. The sequencing depth reached $30\times$ and the mapping rate was higher than 83.6% (Table S6). The sequencing quality was sufficient for further analysis.

A total of 13,136 differentially expressed genes (DEGs) had fpkm > 5 in at least 60% of the samples. We selected 18 as the threshold for module partitioning of WGCNA (Figure 2b). All DEGs were divided into 13 modules. Among them, the turquoise module, where *PmMYB21* is located, has the largest number of DEGs, with 4466 DEGs, accounting for 34.0% of the total DEGs (Figure 2c). This module was significantly positively correlated with the flowering stage of S8 (R = 0.94*, Figure 2d), indicating that genes co-expressed with *PmMYB21* were the main members of DEGs during flowering. Moreover, the enrichment analysis also showed that these genes were mainly involved in biological processes related to flowering, which is consistent with our expectations.
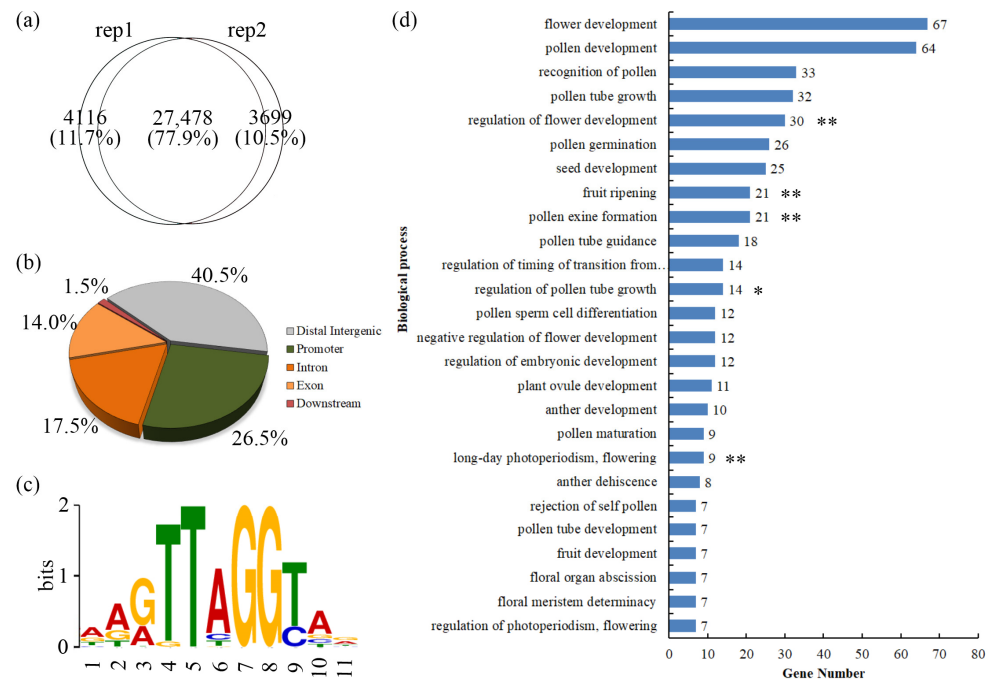

Figure 1. Analysis of the genome-wide binding site of PmMYB21 during flowering stage S6 in mei buds. (**a**) Confidence interval between two replicates. (**b**) Distribution of the locations of predicted binding sites within target genes. Promoter was defined as the sequence within 2 kb upstream of the transcriptional start site; downstream is the sequence within 2 kb downstream of the predicted transcription termination site. (**c**) Motif types of binding regions. (**d**) The flowering-developed processes that the bound genes are mainly involved in, and the number of enriched genes. "*" Indicates Padj < 0.05, "**" Indicates Padj < 0.01.

After validating the transcriptome results using qRT-PCR (Figure S1), we used these co-expressed genes to further screen candidate genes.

3.3. Dap-Seq Combined with WGCNA to Screen Downstream Key Genes of PmMYB21

The genes that Dap-seq detected to be bound by PmMYB21 were identified at DNA level in vitro. This implies that it contains genes that are not actually expressed in the flower buds. On the other hand, RNA-seq was used to detect genes that were specifically expressed in flower buds during flowering. Through WGCNA, we obtained the co-expressed genes of *PmMYB21* in flower buds during flowering, but could not distinguish whether these genes were downstream of *PmMYB21*. By combining Dap-seq and WGCNA, we obtained the downstream genes that had high potential to be directly bound by PmMYB21, and the expression level was positively correlated with flowering. We greatly narrowed down the selection range of candidate genes, and produced 54 candidate genes (Figure 3a). Next, we annotated and listed the expression levels (fpkm values) during flowering, number of binding sites, reference sequences, and identity of these candidate genes (Table S6).
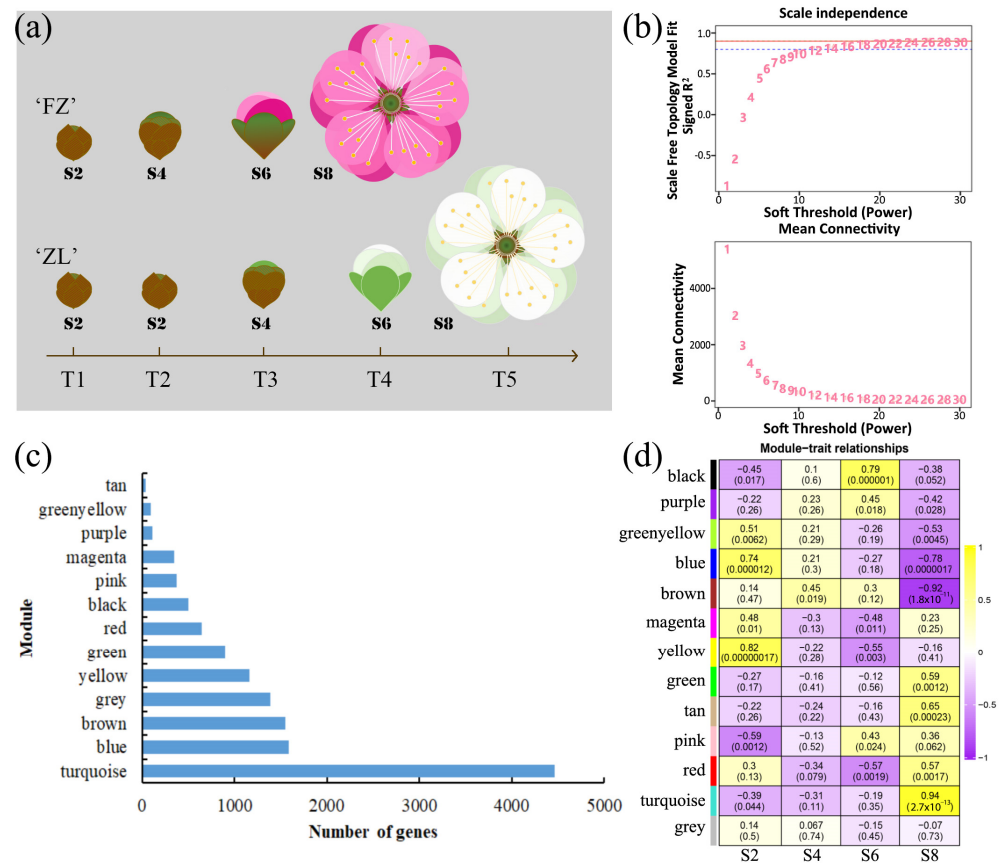
Figure 2. WGCNA of 13,136 DEGs during flowering of two mei cultivars. (**a**) The development of phenological stages of flower buds in mei: bud swelling (S2), sepals clearly visible (S4), petal clearly visible (S6), full blooming (S8). "FZ" and "ZL" indicate *Prunus mume* cultivar "Fenhong Zhusha" and "Zao Lve". (**b**) WGCNA threshold. The blue dashed line and the red line represent R2 = 0.8 and R2 = 0.9, respectively. (**c**) Number of genes in 13 modules. (**d**) The correlation R-value between four key flowering stages and the modules in the analysis of module–phenotype correlation; the number in "()" is the significance *p*-adj value.

After comprehensive consideration, key candidate functional genes were screened out, and their expression trends during flowering were shown using a heat map (Figure 3b). Among 54 candidate genes, 5 MADS-box genes, 10 anther and pollen development genes, 4 auxin signaling genes, and 3 cell wall synthesis genes are included. We are happy to see that MADS-box genes *APETALA1* (*AP1*), *APETALA3* (*AP3*), *SEPALLATA3* (*SEP3*), and *AGAMOUS-LIKE30* (*AGL30*) are in the selected candidate genes. In Arabidopsis, AP1, AP3, PISTILLATA (PI), and SEP interact to form multimeric protein complexes required to specify petal identity [26]. *AGAMOUS* (*AG*) was expressed in pollen to affect stem development, and AGL30 was reported to regulate pollen activity via forms heterodimers with other MICK family members. Auxin response factors 6 (ARF6) mediates auxin response via expression of auxin-regulated genes, and plays an important role in petal and stem development, whereas BT2 mediates responses to nutrients, hormones, and acts during male and female gametophyte development. Most of these genes showed a significant up-regulation trend with the progression of flowering, which was consistent with the significant petal spreading and filament elongation events during this period (Figure 3b).
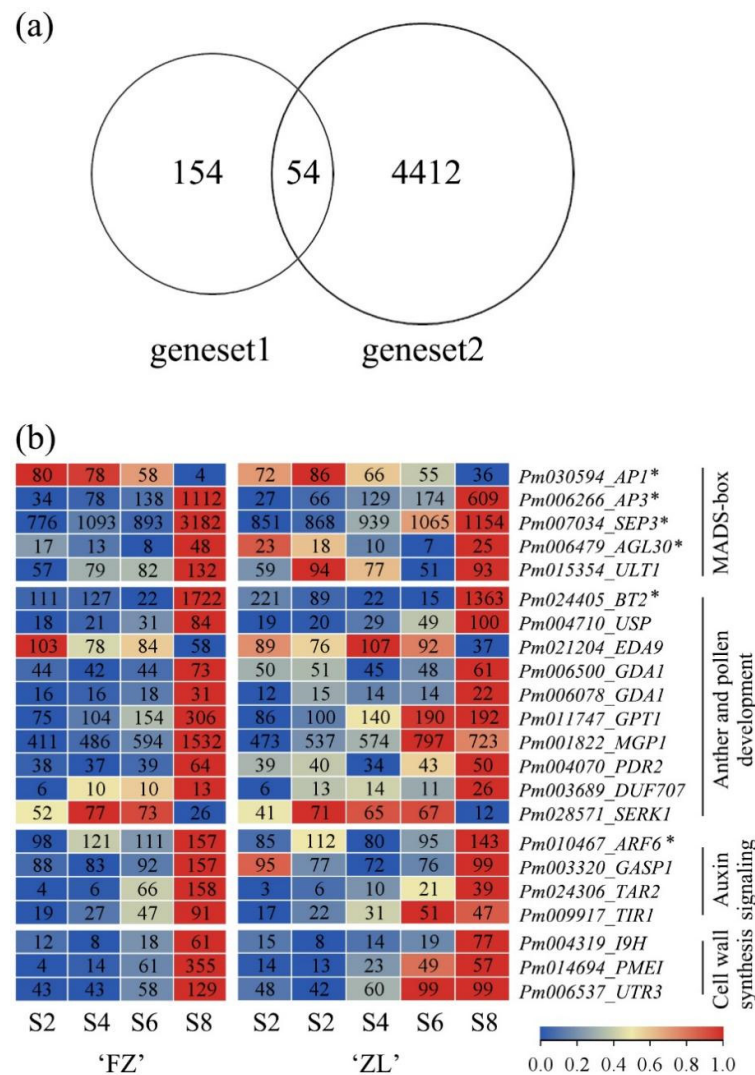
(a)

(b)

80	78	58	4	72	86	66	55	36	*Pm030594_AP1* *	MADS-box
34	78	138	1112	27	66	129	174	609	*Pm006266_AP3* *	
776	1093	893	3182	851	868	939	1065	1154	*Pm007034_SEP3* *	
17	13	8	48	23	18	10	7	25	*Pm006479_AGL30* *	
57	79	82	132	59	94	77	51	93	*Pm015354_ULT1*	
111	127	22	1722	221	89	22	15	1363	*Pm024405_BT2* *	Anther and pollen development
18	21	31	84	19	20	29	49	100	*Pm004710_USP*	
103	78	84	58	89	76	107	92	37	*Pm021204_EDA9*	
44	42	44	73	50	51	45	48	61	*Pm006500_GDA1*	
16	16	18	31	12	15	14	14	22	*Pm006078_GDA1*	
75	104	154	306	86	100	140	190	192	*Pm011747_GPT1*	
411	486	594	1532	473	537	574	797	723	*Pm001822_MGP1*	
38	37	39	64	39	40	34	43	50	*Pm004070_PDR2*	
6	10	10	13	6	13	14	11	26	*Pm003689_DUF707*	
52	77	73	26	41	71	65	67	12	*Pm028571_SERK1*	
98	121	111	157	85	112	80	95	143	*Pm010467_ARF6* *	Auxin synthesis signaling
88	83	92	157	95	77	72	76	99	*Pm003320_GASP1*	
4	6	66	158	3	6	10	21	39	*Pm024306_TAR2*	
19	27	47	91	17	22	31	51	47	*Pm009917_TIR1*	
12	8	18	61	15	8	14	19	77	*Pm004319_I9H*	Cell wall synthesis signaling
4	14	61	355	14	13	23	49	57	*Pm014694_PMEI*	
43	43	58	129	48	42	60	99	99	*Pm006537_UTR3*	
S2	S4	S6	S8	S2	S2	S4	S6	S8		
	'FZ'					'ZL'				

0.0 0.2 0.4 0.6 0.8 1.0

Figure 3. Screening of downstream key candidate genes of PmMYB21. (**a**) Venn plot showing the overlap between geneset1 (the genes high potentially bound by PmMYB21) and geneset2 (co-expressed genes of *PmMYB21*). (**b**) Heatmap of key candidate genes' expression level. "FZ" and "ZL" indicate *Prunus mume* cultivar "Fenhong Zhusha" and "Zao Lve". "*" Indicates key genes.

4. Discussion

In *Arabidopsis thaliana*, MYB21 and its paralogous genes, MYB24 and MYB57, belong to subgroup 19 of R2R3-MYB, which plays an important role in flowering. They are key TFs that control stamens' filament elongation and petal expansion. These TFs are expressed in all four whorls of the flower, with a particular enrichment in stamens [8–11]. *atmyb21*, *atmyb24*, and *atmyb57* single-mutant plants exhibit varying degrees of shorter stamen filaments and delayed anther dehiscence [12]. Those phenotypes were more severe in double mutants than in single mutants. For example, *atmyb21 atmyb24* double mutations lead to short stamen filaments and sterile pollen grains, the anthers cannot dehiscent, and the petals' elongation defects lead to flowers failing to open in Arabidopsis [8,10,12]. The failure of stamen filament elongation was even more serious in the *atmyb21 atmyb24 atmyb57* triple mutant, and petals never grow out of the sepals [8]. In short, MYB21 is the dominant regulator in petal expansion and filament elongation, and AtMYB21/24/57 functions redundantly in regulating the floral organ development [8,10,12]. Few reports exist about the downstream genes of MYB21/24/57. The mechanism of how MYB21 regulates downstream genes and thus the flowering process is still unknown. This is probably related to the difficulty of the redundant regulation of AtMYB21/24/57. Mei, which has non-mosaic

buds, and has only one gene in the 19 subfamily of the R2R3-MYB family, provides special materials for explaining the regulation of MYB21 in the flowering process.

Using Dap-seq, our study examined potential downstream genes of PmMYB21. The proportion of the confidence interval of our results is somewhat higher than that in previous reports, and represents the higher reliability of our results. The promoter region is the main binding region of PmMYB21. This result is consistent with previous reports [27]. There are also examples showing that promoters are not always the most important binding region of TFs [28,29]. This indicates that the binding region preferences of different TFs are diverse. The annotation results showed that the genes bound by PmMYB21 were associated with flower development, anther development, and pollen development. These biological processes are consistent with transcriptome enrichment analysis of flowering processes in other plants [30,31]. Furthermore, DAP-seq sequencing results for MYC-related bHLH proteins indicate that proteins with a similar sequence, such as MYC2, MYC3, MYC4, MYC5, and bHLH17, recognize the same DNA motif, and this pattern is conserved across different species [13]. This implies that our results have significant implications for species with similar PmMYB21 sequences.

We therefore used WGCNA and Veen analysis to further narrow down the candidate geneset, and obtained downstream candidate genes of PmMYB21 that may play a key role during the flowering process of mei. Among the candidate genes, we highlight four TFs, AP1, AP3, and SEP3. Some reports suggest that AP1 is related to flowering time by directly repressing a group of flowering time genes [32]. When *Magnolia wufengensis* experienced winter dormancy and ushered flowering in March, the relative expression of *MawuAP1* increased significantly, which may indicate that AP1 is also involved in the regulation of the environmental temperature response in petal morphogenesis [33]. This expression pattern was the same as that of *PmAP1* during flowering. Previous studies have shown that *PmAP1* is only expressed in the sepals of mei [34]. This may be consistent with our result that *PmAP1* expression levels are gradually down-regulated during flowering, as the calyx no longer grows in the late flowering periods S6 and S8. AP3 could form a heterodimer with PI [35], and then interact with SEP3 to regulate the development of petals and stamens [36–38]. The ectopic expression of *AP3* causes the conversion of the carpel into the stamen structure [39]. In mei, *PmSEP3* was mainly expressed in the flower and fruit. More precisely, the expression level of *PmSEP3* was significantly higher in petals and stamens [34]. SEP3 is also thought to be involved in flowering. The *SEP3*-overexpressing Arabidopsis flowering ignored the low temperature (16 °C), and the number of leaves at flowering was similar to that of the *SEP3*-overexpressing Arabidopsis flowering at 23 °C [40]. This flowering behavior may be related to the bud break and flowering of mei under low temperatures (≤16 °C).

In addition, TFs AGL30, ARF6, and BT1, which also play an important role in flower maturation, were also characterized as PmMYB21 downstream genes. AGL30 belongs to the subset of pollen-specific MIKC-type MADS-box proteins [41]. Previous studies have shown that these proteins bind DNA as heterodimers, which form between S- and P-class MIKC* proteins. While S-class AGL66 and AGL104 lose their function, the pollen of *Arabidopsis thaliana* is low or shows no activity. Among the three heterodimers identified so far, two are heterodimers formed by AGL30 with AGL66, and AGL30 with AGL104, indicating that AGL30 plays a key role in Arabidopsis pollen development [42]. AGL30 was differentially expressed in the anthers of cytoplasmic male sterile *Hibiscus cannabinus* and its maintainer line [43]. There are also reports showing that *AGL30* is preferentially expressed during pollen maturation [41]. This is similar to the expression trend of *PmAGL30* during flowering. ARF6 is mainly expressed in flowers. at*arf6* mutant Arabidopsis has delayed stamen development and decreased fecundity [44]. In *Oryza sativa*, a single mutant of at*arf6* or at*arf12* did not influence the flower opening, and double mutants of at*arf6* and at*arf12* led to failed elongation of the stamen filament [45]. BT1 (BTB and TAZ domain protein 1) is a scaffold protein in the BT family involved in various signaling pathways, and performs a

crucial role in the development of female and male gametophytes [46]. Those phenotypes are consistent with the loss-of-function *myb21* mutant *Arabidopsis*.

5. Conclusions

Flowering is the key event for the ornamental value and fruit production of mei. Our results provide reliable DAP-seq data of PmMYB21, offering a significant reference for future elucidation of the flowering process in mei. Furthermore, by integrating DAP-seq and WGCNA data, our results closely integrated the phenotype, the flowering-specific expression genes, and the regulatory role of PmMYB21. We therefore largely narrowed down the candidate genes and identified a set of key candidate genes that are closely related to the flowering of mei. Considering the conservation of the DNA binding motif among homologous proteins, our findings not only serve as a valuable reference for other fruit trees in Rosaceae, but are also applicable to other species with similar PmMYB21 sequences.

Supplementary Materials: The following supporting information can be downloaded at: https://www.mdpi.com/article/10.3390/f15081300/s1, Figure S1: qRT-PCR results and fpkm values of eight genes; Table S1: Sampling data; Table S2: Primer sequences used for full-length CDs clone and qRT-PCR; Table S3: Dap-seq sequencing basal data; Table S4: Dap-seq promoter GO enrichment_flowering process; Table S5: geneset1 of genes involved in 11 flowering process which could be bound by PmMYB21; Table S6: 54 candidate genes' information.

Author Contributions: X.Y., Y.Z., X.X. and R.H. conceived and designed the experiments. X.Y., H.Z., D.L. (Donghuan Liu) and R.H. performed the experiments. X.Y., R.H., Z.N. and D.L. (Dongyan Liu) analyzed the data. X.Y., Y.Z. and X.X. wrote the manuscript. All authors have read and agreed to the published version of the manuscript.

Data Availability Statement: The original data mentioned in this paper can be found in the National Center for Biotechnology Information (NCBI) repository, PRJNA765446 and PRJNA767019.

Conflicts of Interest: The authors declare no conflicts of interest.

References

1. Chen, J.Y. Origin and history. In *Chinese Mei Flowers*; Chen, J.Y., Ed.; Hainan Publishing House: Haikou, China, 1996; p. 2.
2. Yuan, X.; Ma, K.F.; Zhang, M.H.; Zhang, Z.Y.; Zhang, Q.X. How does an early flowering cultivar of *Prunus mume* arrange its bud development in late winter? *Acta Hortic.* **2020**, *1*, 15–20. [CrossRef]
3. Nishiyama, S.; Matsushita, M.C.; Yamane, H.; Honda, C.; Okada, K.; Tamada, Y.; Moriya, S.; Tao, R. Functional and expressional analyses of apple FLC-like in relation to dormancy progress and flower bud development. *Tree Physiol.* **2021**, *41*, 562–570. [CrossRef]
4. Falavigna, V.D.S.; Guitton, B.; Costes, E.; Andrés, F. I Want to (Bud) Break Free: The Potential Role of DAM and SVP-Like Genes in Regulating Dormancy Cycle in Temperate Fruit Trees. *Front. Plant Sci.* **2018**, *9*, 1990. [CrossRef]
5. Yamane, H.; Kashiwa, Y.; Ooka, T.; Tao, R.; Yonemori, K. Suppression Subtractive Hybridization and Differential Screening Reveals Endodormancy-associated Expression of an SVP/AGL24-type MADS-box Gene in Lateral Vegetative Buds of Japanese Apricot. *J. Am. Soc. Hort. Sci.* **2008**, *133*, 708–716. [CrossRef]
6. Yuan, X.; Zhang, M.; Ma, K.F.; Wang, J.; Zhang, Q.X. Function and Expression Regulation Analysis of *Prunus mume* PmMYB21 During Filament Elongation. *Acta Hortic. Sin.* **2023**, *50*, 1048–1062. [CrossRef]
7. Zhou, C.; Chen, C.; Zuo, J.; Yan, X.; Zhang, J.; Bao, M. Identification and expression analysis of R2R3-MYB transcription factors in *Prunus mume* under cold treatment. *J. Beijing For. Univ.* **2015**, *37*, 5.
8. Cheng, H.; Song, S.; Xiao, L.; Soo, H.M.; Cheng, Z.; Xie, D.; Peng, J. Gibberellin acts through jasmonate to control the expression of MYB21, MYB24, and MYB57 to promote stamen filament growth in Arabidopsis. *PLoS Genet.* **2009**, *5*, e1000440. [CrossRef]
9. Dubos, C.; Stracke, R.; Grotewold, E.; Weisshaar, B.; Martin, C.; Lepiniec, L. MYB transcription factors in Arabidopsis. *Trends Plant Sci.* **2010**, *15*, 573–581. [CrossRef]
10. Mandaokar, A.; Thines, B.; Shin, B.; Lange, B.M.; Choi, G.; Koo, Y.J.; Yoo, Y.J.; Choi, Y.D.; Choi, G.; Browse, J. Transcriptional regulators of stamen development in Arabidopsis identified by transcriptional profiling. *Plant J.* **2006**, *46*, 984–1008. [CrossRef]

11. Shin, B.; Choi, G.; Yi, H.; Yang, S.; Cho, I.; Kim, J.; Lee, S.; Paek, N.C.; Kim, J.H.; Song, P.S.; et al. AtMYB21, a gene encoding a flower-specific transcription factor, is regulated by COP1. *Plant J.* **2002**, *30*, 23–32. [CrossRef]

12. Song, S.; Qi, T.; Huang, H.; Ren, Q.; Wu, D.; Chang, C.; Peng, W.; Liu, Y.; Peng, J.; Xie, D. The Jasmonate-ZIM domain proteins interact with the R2R3-MYB transcription factors MYB21 and MYB24 to affect Jasmonate-regulated stamen development in Arabidopsis. *Plant Cell.* **2011**, *23*, 1000–1013. [CrossRef] [PubMed]

13. López-Vidriero, I.; Godoy, M.; Grau, J.; Peñuelas, M.; Solano, R.; Franco-Zorrilla, J.M. DNA features beyond the transcription factor binding site specify target recognition by plant MYC2-related bHLH proteins. *Plant Commun.* **2021**, *2*, 100232. [CrossRef] [PubMed]

14. Núñez-Lillo, G.; Pérez-Reyes, W.; Riveros, A.; Lillo-Carmona, V.; Rothkegel, K.; Álvarez, J.M.; Blanco-Herrera, F.; Pedreschi, R.; Campos-Vargas, R.; Meneses, C. Transcriptome and Gene Regulatory Network Analyses Reveal New Transcription Factors in Mature Fruit Associated with Harvest Date in Prunus persica. *Plants* **2022**, *11*, 3473. [CrossRef] [PubMed]

15. O'Malley, R.C.; Huang, S.C.; Song, L.; Lewsey, M.G.; Bartlett, A.; Nery, J.R.; Galli, M.; Gallavotti, A.; Ecker, J.R. Cistrome and Epicistrome Features Shape the Regulatory DNA Landscape. *Cell.* **2016**, *165*, 1280–1292. [CrossRef] [PubMed]

16. Bartlett, A.; O'Malley, R.C.; Huang, S.C.; Galli, M.; Nery, J.R.; Gallavotti, A.; Ecker, J.R. Mapping genome-wide transcription-factor binding sites using DAP-seq. *Nat. Protoc.* **2017**, *12*, 1659–1672. [CrossRef] [PubMed]

17. Chen, S.; Zhou, Y.; Chen, Y.; Gu, J. fastp: An ultra-fast all-in-one FASTQ preprocessor. *Bioinformatics.* **2018**, *34*, i884–i890. [CrossRef] [PubMed]

18. Vasimuddin, M.; Sanchit, M.; Heng, L.; Srinivas, A. Efficient Architecture-Aware Acceleration of BWA-MEM for Multicore Systems. In Proceedings of the 2019 IEEE International Parallel and Distributed Processing Symposium (IPDPS), Rio de Janeiro, Brazil, 20–24 May 2019; Available online: https://ieeexplore.ieee.org/document/8820962 (accessed on 2 September 2019).

19. Zhang, Y.; Liu, T.; Meyer, C.A.; Eeckhoute, J.; Johnson, D.S.; Bernstein, B.E.; Nusbaum, C.; Myers, R.M.; Brown, M.; Li, W.; et al. Model-based analysis of ChIP-Seq (MACS). *Genome Biol.* **2008**, *9*, R137. [CrossRef] [PubMed]

20. Machanick, P.; Bailey, T.L. MEME-ChIP: Motif analysis of large DNA datasets. *Bioinformatics.* **2011**, *27*, 1696–1697. [CrossRef] [PubMed]

21. Yu, G.; Wang, L.G.; He, Q.Y. ChIPseeker: An R/Bioconductor package for ChIP peak annotation, comparison and visualization. *Bioinformatics* **2015**, *31*, 2382–2383. [CrossRef] [PubMed]

22. Young, M.D.; Wakefield, M.J.; Smyth, G.K.; Oshlack, A. Gene ontology analysis for RNA-seq: Accounting for selection bias. *Genome Biol.* **2010**, *11*, R14. [CrossRef]

23. Langfelder, P.; Horvath, S. WGCNA: An R package for weighted correlation network analysis. *BMC Bioinform.* **2008**, *9*, 559. [CrossRef]

24. Yuan, X.; Ma, K.; Zhang, M.; Wang, J.; Zhang, Q. Integration of Transcriptome and Methylome Analyses Provides Insight Into the Pathway of Floral Scent Biosynthesis in *Prunus mume*. *Front. Genet.* **2021**, *12*, 779557. [CrossRef] [PubMed]

25. Chen, C.; Chen, H.; Zhang, Y.; Thomas, H.R.; Frank, M.H.; He, Y.; Xia, R. TBtools: An Integrative Toolkit Developed for Interactive Analyses of Big Biological Data. *Mol. Plant* **2020**, *13*, 1194–1202. [CrossRef]

26. Szécsi, J.; Joly, C.; Bordji, K.; Varaud, E.; Cock, J.M.; Dumas, C.; Bendahmane, M. BIGPETALp, a bHLH transcription factor is involved in the control of Arabidopsis petal size. *EMBO J.* **2006**, *25*, 3912–3920. [CrossRef]

27. Mei, F.; Chen, B.; Du, L.; Li, S.; Zhu, D.; Chen, N.; Zhang, Y.; Li, F.; Wang, Z.; Cheng, X.; et al. A gain-of-function allele of a DREB transcription factor gene ameliorates drought tolerance in wheat. *Plant Cell* **2022**, *34*, 4472–4494. [CrossRef]

28. Liu, W.; Zheng, T.; Qiu, L.; Guo, X.; Li, P.; Yong, X.; Li, L.; Ahmad, S.; Wang, J.; Cheng, T.; et al. A 49-bp deletion of PmAP2L results in a double flower phenotype in *Prunus mume*. *Hortic. Res.* **2024**, *11*, uhad278. [CrossRef]

29. Yang, Y.Y.; Shan, W.; Yang, T.W.; Wu, C.J.; Liu, X.C.; Chen, J.Y.; Lu, W.J.; Li, Z.G.; Deng, W.; Kuang, J.F. MaMYB4 is a negative regulator and a substrate of RING-type E3 ligases MaBRG2/3 in controlling banana fruit ripening. *Plant J.* **2022**, *110*, 1651–1669. [CrossRef] [PubMed]

30. Dubois, A.; Remay, A.; Raymond, O.; Balzergue, S.; Chauvet, A.; Maene, M.; Pécrix, Y.; Yang, S.H.; Jeauffre, J.; Thouroude, T.; et al. Genomic approach to study floral development genes in *Rosa* sp. *PLoS ONE* **2011**, *6*, e28455. [CrossRef] [PubMed]

31. Kumar, G.; Gupta, K.; Pathania, S.; Swarnkar, M.K.; Rattan, U.K.; Singh, G.; Sharma, R.K.; Singh, A.K. Chilling Affects Phytohormone and Post-Embryonic Development Pathways during Bud Break and Fruit Set in Apple (Malus domestica Borkh.). *Sci. Rep.* **2017**, *7*, 42593. [CrossRef]

32. Liu, C.; Zhou, J.; Bracha-Drori, K.; Yalovsky, S.; Ito, T.; Yu, H. Specification of Arabidopsis floral meristem identity by repression of flowering time genes. *Development* **2007**, *134*, 1901–1910. [CrossRef]

33. Li, C.; Chen, L.; Fan, X.; Qi, W.; Ma, J.; Tian, T.; Zhou, T.; Ma, L.; Chen, F. *MawuAP1* promotes flowering and fruit development in the basal angiosperm *Magnolia wufengensis* (Magnoliaceae). *Tree Physiol.* **2020**, *40*, 1247–1259. [CrossRef] [PubMed]

34. Xu, Z.; Zhang, Q.; Sun, L.; Du, D.; Cheng, T.; Pan, H.; Yang, W.; Wang, J. Genome-wide identification, characterisation and expression analysis of the MADS-box gene family in *Prunus mume*. *Mol. Genet. Genom.* **2014**, *289*, 903–920. [CrossRef]

35. Riechmann, J.L.; Krizek, B.A.; Meyerowitz, E.M. Dimerization specificity of Arabidopsis MADS domain homeotic proteins APETALA1, APETALA3, PISTILLATA, and AGAMOUS. *Proc. Natl. Acad. Sci. USA* **1996**, *93*, 4793–4798. [CrossRef] [PubMed]

36. Pelaz, S.; Ditta, G.S.; Baumann, E.; Wisman, E.; Yanofsky, M.F. B and C floral organ identity functions require SEPALLATA MADS-box genes. *Nature* **2000**, *405*, 200–203. [CrossRef]

37. Honma, T.; Goto, K. Complexes of MADS-box proteins are sufficient to convert leaves into floral organs. *Nature* **2001**, *409*, 525–529. [CrossRef]

38. Theissen, G. Development of floral organ identity: Stories from the MADS house. *Curr. Opin. Plant Biol.* **2001**, *4*, 75–85. [CrossRef]

39. Jack, T.; Fox, G.L.; Meyerowitz, E.M. Arabidopsis homeotic gene APETALA3 ectopic expression: Transcriptional and posttranscriptional regulation determine floral organ identity. *Cell* **1994**, *76*, 703–716. [CrossRef]

40. Lee, J.H.; Kim, J.J.; Ahn, J.H. Role of SEPALLATA3 (SEP3) as a downstream gene of miR156-SPL3-FT circuitry in ambient temperature-responsive flowering. *Plant Signal Behav.* **2012**, *7*, 1151–1154. [CrossRef]

41. Honys, D.; Twell, D. Transcriptome analysis of haploid male gametophyte development in Arabidopsis. *Genome Biol.* **2004**, *5*, R85. [CrossRef]

42. Adamczyk, B.J.; Fernandez, D.E. MIKC* MADS domain heterodimers are required for pollen maturation and tube growth in Arabidopsis. *Plant Physiol.* **2009**, *149*, 1713–1723. [CrossRef]

43. Li, Z.; Luo, D.; Tang, M.; Cao, S.; Pan, J.; Zhang, W.; Hu, Y.; Yue, J.; Huang, Z.; Li, R.; et al. Integrated Methylome and Transcriptome Analysis Provides Insights into the DNA Methylation Underlying the Mechanism of Cytoplasmic Male Sterility in Kenaf (*Hibiscus cannabinus* L.). *Int. J. Mol. Sci.* **2022**, *23*, 6864. [CrossRef] [PubMed]

44. Nagpal, P.; Ellis, C.M.; Weber, H.; Ploense, S.E.; Barkawi, L.S.; Guilfoyle, T.J.; Hagen, G.; Alonso, J.M.; Cohen, J.D.; Farmer, E.E.; et al. Auxin response factors ARF6 and ARF8 promote jasmonic acid production and flower maturation. *Development* **2005**, *132*, 4107–4118. [CrossRef] [PubMed]

45. Zhao, Z.X.; Yin, X.X.; Li, S.; Peng, Y.T.; Yan, X.L.; Chen, C.; Hassan, B.; Zhou, S.X.; Pu, M.; Zhao, J.H.; et al. miR167d-ARFs Module Regulates Flower Opening and Stigma Size in Rice. *Rice* **2022**, *15*, 40. [CrossRef] [PubMed]

46. Robert, H.S.; Quint, A.; Brand, D.; Vivian-Smith, A.; Offringa, R. BTB and TAZ domain scaffold proteins perform a crucial function in Arabidopsis development. *Plant J.* **2009**, *58*, 109–121. [CrossRef] [PubMed]